Clim. Past Discuss., 7, 4401–4428, 2011
www.clim-past-discuss.net/7/4401/2011/
doi:10.5194/cpd-7-4401-2011

Climate of the Past Discussions

A 500 kyr record of global sea level oscillations in the Gulf of Lion, Mediterranean Sea: new insights into MIS 3 sea level variability

J. Frigola[1], M. Canals[1], I. Cacho[1], A. Moreno[2], F. J. Sierro[3], J. A. Flores[3], S. Berné[4,8], G. Jouet[4], B. Dennielou[4], G. Herrera[1], C. Pasqual[1], J. O. Grimalt[5], M. Galavazi[6], and R. Schneider[7]

[1]CRG Marine Geosciences, Dept. of Stratigraphy, Paleontology and Marine Geosciences, University of Barcelona, Spain
[2]Pyrenean Institute of Ecology, Spanish Research Council, Zaragoza, Spain
[3]Dept. of Geology, University of Salamanca, Spain
[4]IFREMER Laboratoire Environnements Sédimentaires, Plouzané, France
[5]Dept. of Environmental Chemistry, Spanish Research Council, Barcelona, Spain
[6]Fugro Engineers B.V, Leidschendam, The Netherlands

[7]Institut für Geowissenschaften, Christian-Albrechts-Universität zu Kiel, Germany
[8]Université de Perpignan, France

Received: 22 November 2011 – Accepted: 28 November 2011
– Published: 20 December 2011

Correspondence to: M. Canals (miquelcanals@ub.edu)

Published by Copernicus Publications on behalf of the European Geosciences Union.

Abstract

Borehole PRGL1-4 drilled in the upper slope of the Gulf of Lion provides an exceptional record to investigate the impact of Late Pleistocene orbitally-driven glacio-eustatic sea level oscillations on the sedimentary outbuilding of a river fed continental margin. High-resolution grain-size and geochemical records supported by oxygen isotope chronostratigraphy allow reinterpreting the last 500 ka upper slope seismostratigraphy of the Gulf of Lion which consists of five main sequences stacked during the sea level lowering phases of the last five glacial-interglacial 100-kyr cycles. The high sensitivity to sea level oscillations of the grain-size record along the borehole, favoured by the large width of the Gulf of Lion continental shelf, demonstrates that sea level driven changes in accommodation space over the shelf are able to cyclically modify the depositional mode of the entire margin. PRGL1-4 data also illustrate the imprint of sea level oscillations at millennial scale, as shown for Marine Isotopic Stage 3, and provide unambiguous evidence of relative high sea levels at the onset of each Dansgaard-Oeschger Greenland warm interstadial. The PRGL1-4 grain-size record represents the first evidence ever for a one-to-one coupling of millennial-scale sea level oscillations associated with each Dansgaard-Oeschger cycle.

1 Introduction

Sea level oscillations of about 120 m of amplitude paralleled the orbitally-driven 100-kyr climate cycles of the Late Pleistocene in response to global ice volume changes (Imbrie et al., 1992). Jointly with sediment input and subsidence, these sea level oscillations controlled the stratal geometry of passive continental margins where migration of fluvial-influenced deposits generated regressive/transgressive depositional sequences. The seismostratigraphic study of the stacking of those sequences allowed to generate the first approximations to sea level evolution after application of sequential stratigraphy principles (Posamentier and Vail, 1988; Vail et al., 1977). More refined sea level

CPD
7, 4401–4428, 2011

curves have been achieved during the last decades through the measurement of oxygen isotopes on marine sediment cores and dating of coral terraces (Chappell, 2002; Rohling et al., 1998, 2009; Shackleton et al., 2000; Siddall et al., 2003; Thompson and Goldstein, 2005, 2006; Waelbroeck et al., 2002; Yokoyama et al., 2001). However, intrinsic limitations of sea level reconstruction methods and the difficulty of obtaining better and more precise age control of marine records disabled the possibility to accurately constrain orbital and millennial-scale sea level fluctuations. Thus, records from river fed continental margins with very high sedimentation rates and precise chronology of depositional units could provide a better time control and resolution enough to improve reconstruction of past sea level oscillations.

In the Gulf of Lion (GoL) margin, western Mediterranean Sea, deltaic forced Regressive Progradational Units (RPUs) stacked on the outer-shelf and upper slope during relative sea-level falls (Fig. 1), leading some authors to describe this margin as a forced regressive system (Posamentier et al., 1992; Tesson et al., 1990, 2000). The noticeable subsidence rate of the margin, 250 m Myr^{-1} at the shelf edge (Rabineau, 2001), eased the preservation of RPUs in the upper slope as it was continuously submerged even during pronounced lowstands. These conditions allowed the preservation of regressive/transgressive depositional sequences, thus resulting in an ideal area for the study of the Quaternary sedimentary succession. The huge amount of seismic reflection profiles obtained in the GoL margin eased identifying major unconformities defining sequence boundaries in the outer-shelf that become correlative conformities in the upper slope from where five major RPUs were initially described and interpreted to correspond to the last five 100-kyr cycle sea level falls (Fig. 1b) (Bassetti et al., 2008; Rabineau et al., 2005, 1998). However, precise dating of RPUs sequence boundaries was still needed to better constrain the imprint of sea level oscillations on the GoL margin and to determine the leading cyclicity of the deposition of those units, i.e., if they originated during sea level lowerings of 20 or 100 kyr cycles (Lobo et al., 2004).

CPD
7, 4401–4428, 2011

In addition, millennial-scale sea level oscillations at times of rapid climate change during Marine Isotope Stage (MIS) 3 result of special interest since determining their amplitude and phasing is crucial to understand the role of ice sheets on millennial climate variability (Siddall et al., 2008). In fact, MIS 3 relative sea level rises have been tentatively related to both Antarctic and Greenland climate variability (Arz et al., 2007; Rohling et al., 2008; Siddall et al., 2003, 2008; Sierro et al., 2009), which evidences the lack of consensus on the sea level response to rapid climate variability.

Here we present grain-size and geochemical records from a borehole in the GoL upper slope together with a robust oxygen isotope chronostratigraphy, which allow identifying and precisely dating the main RPUs of the last 500 ka, and yield the timing of millennial-scale sea level changes in response to abrupt climate variability during MIS 3.

2 Setting and present day conditions

The GoL forms a crescent-shaped passive margin that is characterized by a wide continental shelf, 70 km of maximum length, covering an area of about 11 000 km^2 (Fig. 1a). The morphology of the continental shelf is mainly derived from the last glacio-eustatic oscillations and post late glacial sedimentation. It includes three main domains: (i) the inner shelf, extending from 0 to 90 m, with soft gradients and parallel and regularly spaced isobaths, also comprising a modern deltaic prism; (ii) the middle shelf, from 90 to 110–120 m, with very low gradient and a rugged morphology, mainly capped by relict offshore sands; and (iii) the outer shelf, from 110–120 m to the shelf break that is characterized again by a smooth morphology (Berné et al., 2004a) (Fig. 1a). The shelf break locates between 120–150 m where numerous submarine canyons cut the margin thus connecting the shelf with the deep basin. This overall morphology confers to the GoL shelf a huge accumulation space for water and sediment storage during periods of relative high sea level, while it remained totally or partly subaerially exposed during past sea level lowerings and lonwstand glacial periods.

CPD
7, 4401–4428, 2011

New insights into MIS 3 sea level variability

J. Frigola et al.

The main source of sediment to the GoL shelf is the Rhone River while other minor fluvial inputs are distributed along the coastline (Pont et al., 2002). Nowadays, all these sediments are mainly trapped in the inner shelf domain, although they can also be reworked and transported offshore by shelf erosive and resuspension processes, mainly driven by the southwestward general circulation pattern of the Northern Current (NC), easterly storms and dense shelf water formation and cascading events (DSWC) (Bassetti et al., 2006; Canals et al., 2006; Dufois et al., 2008; Ulses et al., 2005). In addition to northerly wind-induced DSWC, offshore deep-water formation also takes place during windy winters (Millot, 1999) though with a very low sediment load if compared to major storms and DSWC, both constituting the most effective processes of sediment export from the shelf to the basin mainly through submarine canyons (Canals et al., 2006; Palanques et al., 2006; Pasqual et al., 2010; Sanchez-Vidal et al., 2008).

3 Material and methods

This work is based on the 300 m long continuous sediment core recovered in borehole PRGL1-4 (42°41.39′ N and 03°50.26′ E) drilled at 298 m of water depth in the interfluve separating Aude and Hérault submarine canyons in the GoL during *MV Bavenit* PROMESS1 cruise, and on the 22.77 m long IMAGES core MD99-2348 retrieved at the same location, whose upper 20 m overlap PRGL1-4 (Fig. 1a).

Grain-size analyses on the bulk and the de-carbonated fractions were carried out at 20 cm sampling interval with a Coulter LS 100 Laser Particle Size Analyser after removing organic matter by treatment with excess H_2O_2 and carbonates by treatment with HCl. Grain-size results are discussed here as the silt/clay ratio of the carbonate-free fraction, which relates to energy levels at the time of particle deposition (Frigola et al., 2007). Matching of silt/clay ratio records from both fractions allows discarding the in-situ paleoproductivity signal to affect the grain-size record (Fig. 2b).

Semi-quantitative analysis of major elements (Ca, Fe, Ti and K) was carried out at 4 cm resolution using the first generation Avaatech non-destructive X-ray fluorescence

(XRF) core scanner of the University of Bremen. Here we present the Ca record as the main indicative of fluvial inputs to the GoL since variability from all of the XRF-elements is related to oscillations in Ca supply, mainly derived from the fluvial discharge of fines.

The age model was obtained by synchronizing the records of *Globigerina bulloides* δ^{18}O and abundance of temperate to warm planktic foraminifers to the North GRIP ice core isotope record for the last 120 ka (Andersen et al., 2006; NGRIP, 2004; Svensson et al., 2008). From 120 to 530 ka the age model was built by aligning the PRGL1-4 *G. bulloides* δ^{18}O record to the SPECMAP isotope stack (Martinson et al., 1987). For more details on the age model, tie points and ^{14}C-AMS dates see Sierro et al. (2009) and Table 1. Temporal variability of sedimentation rates (SR) resulted in a mean temporal resolution of 160 and 1550 yr during glacial and interglacial periods, respectively.

4 Results and discussion

4.1 The orbital 100-kyr sea level imprint

The silt/clay ratio and Ca records from PRGL1-4 show a seesaw pattern defining five main units characterized by an upwards fining and Ca content increasing trend, which nicely correlate with the main seismostratigraphic units (Fig. 2). The sedimentary units end with an abrupt increase in the silt/clay ratio and a rapid decrease in the Ca content coinciding with the main reflectors corresponding to sequence boundaries in the seismic reflection profile. The excellent correlation of these analytical sequences with the seismostratigraphy, together with chronostratigraphy from the *G. bulloides* δ^{18}O record (Sierro et al., 2009), confirms the 100-kyr-cycle origin of these units. The data derived from PRGL1-4 borehole allowed reinterpreting the seismostratigraphy of the GoL upper slope, where seven units (S1, S2a, S2b, S3a, S3b, S4 and S5) are now documented (Jouet, 2007) instead of the five (S1 to S5) previously identified from seismic reflection profiles only (Rabineau, 2001). The seven units result from decomposition of former sequences S2 and S3 into S2a and S2b, and S3a and S3b, respectively (Fig. 2a). The lowermost seismostratigraphic units S1 and S2a were not penetrated at PRGL1-4, and our results suggest that the base of the drill likely correspond to MIS 13 while Termination VI (TVI) was not reached (Fig. 2d). Accordingly, the top five major depositional sequences stacked on the upper slope of the GoL, corresponding to RPUs driven by global sea level oscillations of the last five glacial cycles, are perfectly identified in the continuous sedimentary record of PRGL1-4 borehole. Abrupt increases in the silt/clay ratio and decreases in the Ca content respond to rapid sea level rise, continental shelf flooding and subsequent landward migration of deltaic systems during glacial-interglacial transitions giving birth to sequence boundaries in the upper slope (Fig. 2).

RPU stacking in the upper slope resulted from seaward migration of deltaic systems and the subsequent enhancement of riverine supply because of the sea level lowering during each 100-kyr cycle. That is why maximum sedimentation rates (1.5–2.5 $m\,kyr^{-1}$) in the upper slope were recorded during periods when the distance to river mouths was minimal (i.e. during glacial lowstands) (Figs. 3f and 4a). The presence of relict offshore sands at 110–115 m depth along the outermost shelf further supports the location of lowstand glacial paleo-shorelines in the vicinity of the Aude Canyon head (Aloïsi, 1986; Bassetti et al., 2006; Berné et al., 2004a; Jouet et al., 2006). The increasing trend of SRs paralleling sea level lowering across a glacial period is particularly well resolved for the last glacial period (MIS 2, 3 and 4) thanks to the robustness of the chronostratigraphic control (Fig. 3f). Sedimentation rates also peaked during previous 100-kyr cycles glacial sea level minima, although the reduction in chronostratigraphic control with depth does not allow distinguishing SR trends during previous full forced regressions, but only low or high SR during interglacial and glacial periods, respectively. Co-occurrence of lowest silt/clay ratios and highest Ca contents during glacial sea level minima confirms the reinforced influence of nearby glacial river mouths on the sedimentation of fines over the upper slope interfluve (Fig. 3c,e). Accordingly, while during glacial lowstands the coarsest fractions were mostly trapped and funnelled by glacial

CPD
7, 4401–4428, 2011

adjacent submarine canyons, as demonstrated by pronounced axial incisions within their upper courses (Baztan et al., 2005), large amounts of fine particles supplied by the nearby river mouths remained in suspension un-trapped by the canyons and leading to substantial accumulation in inter-canyon areas (i.e. the interfluves).

In contrast, SRs were lowest (0.10–0.25 m kyr^{-1}) at interglacial sea level highstands associated with the landward migration of deltaic systems far away from the shelf-break and upper slope (Figs. 3f and 4b), as illustrated by the modern Holocene epicontinental prism extending down to 90 m water depth over the inner shelf (Aloïsi, 1986; Berné et al., 2007, 2004b). Obviously, these contrasting sedimentation rates resulted in expanded glacial intervals (i.e. with higher temporal resolution) and condensed interglacial intervals along our 500 kyr record (Fig. 3). That means that with each sea level rise, sedimentation rates reduce significantly in the upper slope and PRGL1-4 records lose time resolution (e.g. just few points represent a full interglacial period). In addition, the very low SRs during the main interglacial highstands led to the formation of condensed layers (CLs), i.e. sandy layers rich in pelagic skeletal material, along the GoL upper slope (Fig. 3d), as shown by the total fine sand record of Sierro et al. (2009).

However, the landward excursion of deltaic systems pushed by sea level rise and the associated reduction in sediment flux to the upper slope during glacial/interglacial transitions do not explain by themselves the sustained supply of coarse particles to the upper-slope during all interglacial periods as evidenced by the elevated silt/clay ratio (Fig. 3c) nor the observed increase in sand particles into the carbonate-free fraction (mainly quartz grains). Then, it is probable that the interglacial flooding of the 70 km wide GoL shelf (Fig. 4b) reactivated oceanographic processes able to erode, resuspend and transport coarse particles, lilkely contributing to the formation of CLs. While the southwards flowing Northern Current (NC) sweeping the shelf edge and upper slope (Fig. 1a) could contribute to winnow the finest particles during long lasting periods of reduced sediment input to the upper slope, it could not explain the arrival of new lithic coarse material found in CLs and, more generally, in deposits formed during interglacial periods. The inundation of the shelf during interglacial periods generated

CPD
7, 4401–4428, 2011

a relatively thin layer of water that was highly sensitive to atmospheric forcings, which may trigger the remobilisation of sedimentary particles temporarily stored on the shelf, as it happens during the present day highstand (Bassetti et al., 2006; Canals et al., 2006; Dufois et al., 2008). Recent studies have demonstrated that nowadays northern cold, strong and persistent winds lead to DSWC down-slope at high speed (up to $1\,\mathrm{m\,s^{-1}}$ or more) during late winter and early spring months in the GoL (Canals et al., 2006). Cascading waters carry large amounts of organic matter and sedimentary particles whose coarser fraction efficiently scours and erodes the shelf edge and canyon heads and upper courses (Gaudin et al., 2006; Lastras et al., 2007; Pasqual et al., 2010; Puig et al., 2008; Sanchez-Vidal et al., 2008). Activation in the past of continental shelf erosive processes like DSWC probably did not lead to significant sediment accumulation in upper slope interfluves but favoured the winnowing of fines and the supply of coarse lithic particles that, in combination with low sedimentation rates, contributed to generate CLs. When the "cooling platform" disappeared, i.e. during subaerial exposure of the continental shelf (lowstand conditions, Fig. 4a), there was no room left for dense shelf waters to form and, therefore, this type of continental shelf erosive processes ceased. During transitional periods, when the shelf was partly flooded, the volume of water involved in cascading and other continental shelf erosive processes was smaller, subsequently lessening downslope transport by dense shelf waters. Therefore, changes in the silt/clay ratio also respond to the flooded shelf area and, consequently, to sea level oscillations. This explains the relatively good matching between the silt/clay ratio and sea level for the last 500 ka (Fig. 3a,c), which is especially evident for the last glacial cycle where the chronostratigraphic control is more precise. Obviously, the silt/clay ratio did not respond linearly to sea level oscillations and reactivation of continental shelf erosive processes could be also related to some environmental threshold, e.g. the volume of water stored on the shelf. This, together with significant reductions of SRs during each sea level rise, and subsequent reductions in time resolution, prevent us to use the silt/clay ratio as an exact indicator of the beginning of sea level rises. However, the persistent pattern observed in the silt/clay

CPD
7, 4401–4428, 2011

ratio through the last five glacial/interglacial cycles and also at millennial time scales, as described below, confirms this ratio is a good indicator of relative high sea level conditions (highstands) in the GoL margin.

These results support a shelf and upper slope depositional model for inter-canyon RPU stacking over the last 500 ka that considers two main processes: (i) oscillations in sediment supply due to the migration of river mouths and deltaic systems and, (ii) activation-deactivation of continental shelf erosive processes like DSWC, both of them ultimately driven by the 100-kyr glacio-eustatic cycle (Fig. 4).

4.2 The millennial MIS 3 sea level imprint

Since this combined depositional model has been working at glacial/interglacial scales, it is reasonable to expect that minor scale sea level oscillations would result in some sort of sedimentary signature in the GoL margin outbuilding too. Taking into account the passive character of the margin, the flatness and width of the GoL shelf, and the robust chronostratigrafic frame for the last glacial cycle (i.e. excellent synchronization between the PRGL1-4 *G. bulloides* δ^{18}O record and the NGRIP ice core record, Fig. 5a and B) due to elevated SRs (ranging from 0.2 to 2 m kyr^{-1}), the PRGL1-4 record could be highly valuable to disentangle the millennial scale sea level variability during MIS 3. Independently of chronologies, the exhaustive compilation of MIS 3 sea level reconstructions by Siddall et al. (2008) shows two common patterns of variability: (1) the mean sea level during the first half of MIS 3 was approximately 20 m higher than in the second half, and (2) four 20–30 m in amplitude millennial-scale sea level fluctuations occurred during this period (Fig. 5e). These features are also observed in the PRGL1-4 silt/clay record (Fig. 5c), thereby demonstrating that the GoL system responded to both long and short-term sea level fluctuations during MIS 3.

The general decreasing trend observed in the PRGL1-4 silt/clay ratio during the progressive sea level lowering of the last glacial cycle (Fig. 3), is punctuated by a series of grain-size increases, which suggest that millennial-scale relative sea level rises

CPD
7, 4401–4428, 2011

occurred during MIS 3 (Fig. 5c). By temporally extending the flooded area of the GoL shelf, MIS 3 relative sea level rises reduced the clay supply to the upper slope and contributed to expose a larger volume of water to atmospheric forcing, eventually leading to DSWC and hence indirectly reinforcing the transport of coarse particles to the upper slope. Both mechanisms contributed to increases in the silt/clay ratio (Fig. 5c). Those grain-size increases are unrelated to periods of intensification of deep-water formation in the GoL since most of them occured during relatively warm Greenland interstadials (GIS) (Fig. 5c,b), in contrast with observations of enhanced Western Mediterranean Deep Water (WMDW) formation during MIS 3 cold Greenland Stadials (GS) (Cacho et al., 2000, 2006; Frigola et al., 2008; Sierro et al., 2005).

Confirming or discarding the occurrence of sea level oscillations at Dansgaard-Oeschger (D/O) scale has been prevented so far because none of the existing sea level records was able to resolve variations lower than 12 m in amplitude during time intervals as short as 1 kyr (Siddall et al., 2008). Nevertheless, prominent increases in iceberg calving during cold Greenland stadials (GS) (non Heinrich events, HE) suggest that sea level should have oscillated within each D-O cycle (Bond and Lotti, 1995; Chappell, 2002; Siddall et al., 2008; van Kreveld et al., 2000). Disentangling MIS 3 sea level variability also faces the difficulty to establish the absolute timing of the observed oscillations, which is necessary to understand the role of sea level in millennial-scale climate variability during MIS 3 and to determine the relative contribution of “northern” versus “southern” sources (Clark et al., 2007).

Early evidence of millennial-scale sea level variability were obtained from the benthic δ^{18}O record of Portuguese margin core MD95-2042 (Shackleton et al., 2000), that although may be influenced by oscillations in deep ocean temperature and local hydrographic variability an important part of the record is linked to global sea level change (Skinner et al., 2007), and sea level reconstruction from the Red Sea (Siddall et al., 2003) (Fig. 5e). Since both records display a variability pattern remarkably similar to the one found in Antarctic ice cores (Fig. 5g), it has been suggested that MIS 3 sea level oscillations followed Antarctic climate variability (Rohling et al., 2008; Siddall et al.,

CPD
7, 4401–4428, 2011

2003). Contrary to these interpretations, recent results from the Red Sea and the GoL have shown millennial-scale sea level rises to occur during major warm Greenland interstadials (GIS) (Fig. 5f and d) (Arz et al., 2007; Jouet et al., 2011; Sierro et al., 2009), further highlighting the still high uncertainty about the timing of MIS 3 sea level variability.

The co-occurrence of silt/clay increases and planktic δ^{18}O depletions in the PRGL1-4 record (Fig. 5c,b) imply, independently of the age model applied, that relative high sea levels occurred during warm GIS events. Concurrently, Shackleton et al. (2000) and Siddall et al. (2003) records also show maximum sea levels to occur during the onset phase of major GIS interstadials (i.e. GIS14, 12 and 8) (Fig. 5e). However, discrepancies on the precise time of the sea level rises exist with our PRGL1-4 record. The excellent time constrain provided by the *G. bulloides* δ^{18}O record of the PRGL1-4 borehole demonstrates a perfect peak to peak coupling between sea level variability (as indicated by increases in the silt/clay ratio) and all D-O cycles, including the shortest ones. Nevertheless, not every relative high sea level resulted in the formation of CLs since these were only observed during major GIS (16, 14, 12, 8 and 7) (Sierro et al., 2009), all of which coincide with higher values of the silt/clay ratio (Fig. 5d,c). The differences between the total fine sand record of Sierro et al. (2009) and our silt/clay ratio indicate that sea level increases during minor GIS (15, 13, 11, 10, 9, 6, 5, 4 and 3) were likely not high and/or long enough to generate CLs, therefore demonstrating once more the strong sensitivity of the silt/clay ratio to sea level oscillations.

A limitation of the PRGL1-4 silt/clay record is that the amplitude of sea level variations cannot be directly derived as nowhere is proven that grain-size oscillations respond linearly to sea level fluctuations. This very same limitation, and reduction of PRGL1-4 time resolution due to decreasing SRs with sea level increases, also prevents setting up the precise timing of sea level rises whether they occurred at the beginning of each warm GIS or during the previous cold stadial. This relates to the exact time of deltaic migration and their relative position following sea level rise. In addition, the enhanced supply of coarse particles by reactivation of continental shelf erosive processes, such

CPD
7, 4401–4428, 2011

as DSWC, should normally occur some time after the start of each sea level rise, i.e. when the volume of water over the shelf is again large enough.

Our results imply that sea level was relatively high during all warm GIS within MIS 3 (Fig. 5c,a), although intrinsic limitations of the methodology applied in this study do not allow establishing the precise time nor the mechanism of such millennial scale sea level rises, which could initiate by instabilities and melting of continental ice-sheets during cold GS, whether or not they correspond to HEs.

5 Conclusions

The last 500 ka continuous sediment record of the 300 m long PRGL1-4 borehole drilled in the upper slope of the river fed GoL holds the imprint of sea level oscillations at orbital and millennial time scales. The sedimentary succession of PRGL1-4 consists of five regressive progradational units that relate to the glacio-eustatic 100-kyr cyclicity. The consistent chronostratigraphy of the investigated section and the perfect matching between seismic reflection profiles and the grain-size record provide clues to understand the nature of seismic reflections in mud-dominated slope sequences like the ones found at the investigated site and also provides a tool to identify and precisely locate the boundaries of seismostratigraphic units while helping to tie them with global sea level oscillations. This resulted in a reinterpretation of the stratigraphy of the upper slope in the GoL following an approach that can be extended to similar continental margin settings.

In addition of pushing the shoreline and associated sedimentary environments landwards, thus disconnecting the upper slope from direct riverine sediment sources, we have demonstrated that sea level rise can reactivate transient energetic hydrosedimentary processes, such as DSWC, which are able of eroding, resuspending and transporting large volumes of sediment from the continental shelf and upper slope to the deep basin. The sedimentary starvation of the upper slope during highstands, jointly with both episodic and persistent hydrodynamic processes winnowing the fine fraction,

CPD
7, 4401–4428, 2011

determined the formation of CLs that mark the periods of continental shelf flooding during interglacial epochs, as evidenced by our grain-size records.

Finally, the excellent match of the PRGL1-4 silt/clay record with previous records of sea level variability at millennial-scale during MIS 3, together with the good time constrain provided by the *G. bulloides* δ^{18}O record, strongly support the occurrence of relatively high sea levels during each single warm GIS, even the smallest ones. Unfortunately, the precise starting time of sea level rises cannot be established solely from the sediment record of the upper slope GoL, which points to the need of further devoted research to resolve the origin and magnitude of MIS 3 sea level variability.

Acknowledgements. This study has been supported by the EC PROMESS1 (EVR1-CT-200240024), HERMIONE (226354-HERMIONE) and SESAME (Prop. Number: 036949-2) projects, and the Spanish GRACCIE CONSOLIDER (CSD2007-00067) and DOS MARES (CTM2010-21810-C03-01) projects and CGL2005-24147-E complementary action. The IMAGES programme contributed to the research by providing the MD99–2348 sediment core. French partners benefited from additional support by Agence Nationale de la Recherche (ANR, contract NT05-3-42040). We thank Anders Sevensson and Thomas Blunier for providing NGRIP and EDML data, respectively. We are especially grateful to PROMESS1 participating scientists and to the staff of the various laboratories where the sediment samples were analyzed. We are grateful for the support provided by Fugro Engineers B.V. that made the challenging *MV Bavenit* cruise a success history. Generalitat de Catalunya recognizes CRG Marine Geosciences within its excellence research groups program (ref. 2009 SGR 1305).

References

Aloïsi, J. C.: Sur un Modèle de Sédimentation Deltaïque: Contribution à la Connaissance des Marges Passives, University of Perpignan, Perpignan, pp. 162, 1986.

Andersen, K. K., Svensson, A., Johnsen, S. J., Rasmussen, S. O., Bigler, M., Rothlisberger, R., Ruth, U., Siggaard-Andersen, M.-L., Peder Steffensen, J., Dahl-Jensen, D., Vinther, B. M., and Clausen, H. B.: The Greenland ice core chronology 2005, 15–42 ka. Part 1: constructing the time scale, Quaternary Sci. Rev., 25, 3246–3257, 2006.

Arz, H. W., Lamy, F., Ganopolski, A., Nowaczyk, N., and Patzold, J.: Dominant Northern Hemisphere climate control over millennial-scale glacial sea-level variability, Quaternary Sci. Rev., 26, 312–321, 2007.
Bassetti, M. A., Jouet, G., Dufois, F., Berne, S., Rabineau, M., and Taviani, M.: Sand bodies at the shelf edge in the Gulf of Lions (Western Mediterranean): deglacial history and modern processes, Mar. Geol., 234, 93–109, 2006.
Bassetti, M. A., Berné, S., Jouet, G., Taviani, M., Dennielou, B., Flores, J. A., Gaillot, A., Gelfort, R., Lafuerza, S., and Sultan, N.: The 100-ka and rapid sea level changes recorded by prograding shelf sand bodies in the Gulf of Lions (Western Mediterranean Sea), Geochem. Geophys. Geosyst., 9, Q11R05, doi:10.1029/2007GC001854, 2008.
Baztan, J., Berne, S., Olivet, J. L., Rabineau, M., Aslanian, D., Gaudin, M., Rehault, J. P., and Canals, M.: Axial incision: The key to understand submarine canyon evolution (in the Western Gulf of Lion), Mar. Petrol. Geol., 22, 805–826, 2005.
Berné, S., Carré, B., Loubrieu, B., Mazé, J. P., Morvan, L., and Normand, A.: Notice de la carte morpho-bathymétrique du Golfe du Lion, IFREMER, Brest, 2004a.
Berné, S., Rabineau, M., Flores, J. A., and Sierro, F. J.: The impact of Quaternary Global Changes on strata formation. Exploration of the shelf edge in the Northwest Mediterranean Sea, Oceanography, 17, 92–103, 2004b.
Berné, S., Jouet, G., Bassetti, M. A., Dennielou, B., and Taviani, M.: Late glacial to preboreal sea-level rise recorded by the Rhone deltaic system (NW Mediterranean), Mar. Geol. 245, 65–88, doi:10.1016/j.margeo.2007.07.00, 2007.
Blunier, T. and Brook, E. J.: Timing of millennial-scale climate change in Antarctica and Greenland during the last glacial period, Science, 291, 109–112, 2001.
Bond, G. and Lotti, R.: Iceberg discharges into the North Atlantic on millennial time scales during the last deglaciation, Science, 267, 1005–1010, 1995.
Cacho, I., Grimalt, J. O., Sierro, F. J., Shackleton, N. J., and Canals, M.: Evidence for enhanced Mediterranean thermohaline circulation during rapid climatic coolings, Earth Planet. Sci. Lett., 183, 417–429, 2000.
Cacho, I., Shackleton, N., Elderfield, H., Sierro, F. J., and Grimalt, J. O.: Glacial rapid variability in deep-water temperature and δ^{18}O from the Western Mediterranean Sea, Quaternary Sci. Rev., 25, 3294–3311, 2006.
Canals, M., Puig, P., de Madron, X. D., Heussner, S., Palanques, A., and Fabres, J.: Flushing submarine canyons, Nature, 444, 354–357, 2006.

Clark, P. U., Hostetler, S. W., Pisias, N. G., Schmittner, A., and Meissner, K.: Mechanisms for an ∼7-kyr climate and sea-level oscillation during Marine Isotopic Stage 3, in: Ocean Circulation: Mechanisms and Impacts, edited by: Schmittner, A., Chiang, J. C. H., and Hemming, S. R., AGU Geophysical Monograph Series, 173, Washington, D. C., 209–246, 2007.

Chappell, J.: Sea level changes forced ice breakouts in the Last Glacial cycle: new results from coral terraces, Quaternary Sci. Rev. 21, 1229–1240, 2002.

Dufois, F., Garreau, P., Le Hir, P., and Forget, P.: Wave- and current-induced bottom shear stress distribution in the Gulf of Lions, Cont. Shelf Res., 28, 1920–1934, 2008.

EPICA Community Members: One-to-one coupling of glacial climate variability in Greenland and Antarctica, Nature 444, 195–198, 2006.

Frigola, J., Moreno, A., Cacho, I., Canals, M., Sierro, F. J., Flores, J. A., Grimalt, J. O., Hodell, D. A., and Curtis, J. H.: Holocene climate variability in the Western Mediterranean region from a deepwater sediment record, Paleoceanography, 22, PA2209, doi:10.1029/2006PA001307, 2007.

Frigola, J., Moreno, A., Cacho, I., Canals, M., Sierro, F. J., Flores, J. A., and Grimalt, J. O.: Evidence of abrupt changes in Western Mediterranean deep water circulation during the last 50 kyr: a high-resolution marine record from the Balearic Sea, Quaternary Int., 181, 88–104, doi:10.1016/j.quaint.2007.06.016, 2008.

Gaudin, M., Berne, S., Jouanneau, J. M., Palanques, A., Puig, P., Mulder, T., Cirac, P., Rabineau, M., and Imbert, P.: Massive sand beds attributed to deposition by dense water cascades in the Bourcart canyon head, Gulf of Lions (Northwestern Mediterranean Sea), Mar. Geol., 234, 111–128, doi:10.1016/j.margeo.2006.09.020, 2006.

Imbrie, J., Boyle, E., Clemens, C., Duffy, A., Howard, W., Kukla, G., Kutzbach, J. E., Martinson, D. G., McIntyre, A., Mix, A. C., Molfino, B., Morley, J. J., Peterson, L. C., Pisias, N. G., Prell, W., Raymo, M. E., Shackleton, N. J., and Toggweiler, J. R.: On the structure and origin of major glaciation cycles. 1. Linear responses to Milankovitch forcing, Paleoceanography, 7, 701–738, 1992.

Jouet, G.: Enregistrements Stratigraphiques des Cycles Climatiques et Glacio-eustatiques du Quaternaire Terminal-Modélisations de la Marge Continentale du Golfe du Lion, Laboratoire Environnements Sédimentaires, Géosciences Marines, Ifremer, Brest, France, pp. 443, 2007.

Jouet, G., Berne, S., Rabineau, M., Bassetti, M. A., Bernier, P., Dennielou, B., Sierro, F. J., Flores, J. A., and Taviani, M.: Shoreface migrations at the shelf edge and sea-level changes

CPD

7, 4401–4428, 2011

around the Last Glacial Maximum (Gulf of Lions, NW Mediterranean), Mar. Geol., 234, 21–42, 2006.
Jouet, G., Berné, S., Sierro, F. J., Bassetti, M. A., Canals, M., Dennielou, B., Flores, J. A., Frigola, J., and Haq, B. U.: Geological imprints of millennial-scale sea-level changes, Terra Nova, accepted, 2011.
van Kreveld, S. A., Sarnthein, M., Erlenkeuser, H., Grootes, P., Jung, S. J. A., Nadeau, M.-J., Pflaumann, U., and Voelker, A.: Potential links between surging ice sheets, circulation changes, and the Dansgaard-Oeschger cycles in the Irminger Sea, 60–18 kyr, Paleoceanography, 15, 425–442, 2000.
Lastras, G., Canals, M., Urgeles, R., Amblas, D., Ivanov, M., Droz, L., Dennielou, B., Fabrés, J., Schoolmeester, T., Akhmetzhanov, A., Orange, D., and García-García, A.: A walk down the Cap de Creus canyon, Northwestern Mediterranean Sea: recent processes inferred from morphology and sediment bedforms, Mar. Geol., 246, 176–192, 2007.
Lobo, F. J., Tesson, M., and Gensous, B.: Stratral architectures of late quaternary regressive-transgressive cycles in the Roussillon Shelf (SW Gulf of Lions, France), Mar. Petrol. Geol., 21, 1181–1203, 2004.
Martinson, D. G., Pisias, N. G., Hays, J. D., Imbrie, J., Moore, T. C., and Shackleton, N.: Age dating and the orbital theory of the ice ages: development of a high-resolution 0 to 300 000-years chronostratigraphy, Quaternary Res., 27, 1–29, 1987.
Millot, C.: Circulation in the Western Mediterranean Sea, J. Mar. Syst., 20, 423–442, 1999.
NGRIP: High-resolution record of Northern Hemisphere climate extending into the last interglacial period, Nature, 431, 147–151, 2004.
Palanques, A., Durrieu de Madron, X., Puig, P., Fabres, J., Guillen, J., Calafat, A., Canals, M., Heussner, S., and Bonnin, J.: Suspended sediment fluxes and transport processes in the Gulf of Lions submarine canyons. The role of storms and dense water cascading, Mar. Geol., 234, 43–61, 2006.
Pasqual, C., Sanchez-Vidal, A., Zúñiga, D., Calafat, A., Canals, M., Durrieu de Madron, X., Puig, P., Heussner, S., Palanques, A., and Delsaut, N.: Flux and composition of settling particles across the continental margin of the Gulf of Lion: the role of dense shelf water cascading, Biogeosciences, 7, 217–231, doi:10.5194/bg-7-217-2010, 2010.
Pont, D., Simonnet, J. P., and Walter, A. V.: Medium-term changes in suspended sediment delivery to the ocean: consequences of catchment heterogeneity and river management (Rhône River, France), Estuar. Coast. Shelf S., 54, 1–18, 2002.

Posamentier, H. W. and Vail, P. R.: Eustatic controls on clastic deposition II – sequence and systems tract models, in: Sea-Level Changes: an Integrated Approach, edited by: Wilgus, C. K., Hastings, B. S., Kendall, C. G. S. C., Posamentier, H., Ross, C. A., Van and Wagoner, J. C., Society of Economic Paleontologists and Mineralogists, Tulsa, 125–154, 1988.

Posamentier, H. W., Allen, G. P., James, D. P., and Tesson, M.: Forced regressions in a sequence stratigraphic framework: concepts, examples, and exploration significance, Am. Assoc. Petrol. Geol. (AAPG) B., 76, 1687–1709, 1992.

Puig, P., Palanques, A., Orange, D. L., Lastras, G., and Canals, M.: Dense shelf water cascades and sedimentary furrow formation in the Cap de Creus Canyon, Northwestern Mediterranean Sea, Cont. Shelf Res., 28, 2017–2030, 2008.

Rabineau, M.: Un modèle géométrique et stratigraphique des séquences de dépôts quaternaires de la plate-forme du Golfe du Lion: enregistrement des cycles glacioeustatiques de 100 000 ans, Thèse de Doctorat. Université de Rennes 1 and IFREMER, Rennes, pp. 392 + 370, vol. 392, available at: http://archimer.ifremer.fr/doc/00000/331/, 2001.

Rabineau, M., Berné, S., Ledrezen, E., Lericolais, G., Marsset, T., and Rotunno, M.: 3-D architecture of lowstand and transgressive Quaternary sand bodies on the outer shelf of the Gulf of Lion, France, Mar. Petrol. Geol., 15, 439–452, 1998.

Rabineau, M., Berne, S., Aslanian, D., Olivet, J.-L., Joseph, P., Guillocheau, F., Bourillet, J.-F., Ledrezen, E., and Granjeon, D.: Sedimentary sequences in the Gulf of Lion: a record of 100 000 years climatic cycles, Mar. Petrol. Geol., 22, 775–804, 2005.

Rohling, E. J., Fenton, M., Jorissen, F. J., Bertrand, P., Ganssen, G., and Caulet, J. P.: Magnitudes of sea-level lowstands of the past 500 000 years. Nature, 394, 162–165, 1998.

Rohling, E. J., Grant, K., Hemleben, C., Kucera, M., Roberts, A. P., Schmeltzer, I., Schulz, H., Siccha, M., Siddall, M., and Trommer, G.: New constrains on the timing of sea level fluctuations during early to middle isotope stage 3, Paleoceanography, 23, PA3219, doi:10.1029/2008PA001617, 2008.

Rohling, E. J., Grant, K., Bolshaw, M., Roberts, A. P., Siddall, M., Hemleben, C., and Kucera, M.: Antarctic temperature and global sea level closely coupled over the past five glacial cycles, Nat. Geosci., 2, 500, 2009.

Sanchez-Vidal, A., Pasqual, C., Kerhervé, P., Calafat, A., Heussner, S., Palanques, A., Durrieu de Madron, X., Canals, M., and Puig, P.: Impact of dense shelf water cascading on the transfer of organic matter to the deep Western Mediterranean basin, Geophys. Res. Lett., 35, L05605, doi:10.1029/2007GL032825, 5, 2008.

CPD
7, 4401–4428, 2011

Shackleton, N. J., Hall, M. A., and Vincent, E.: Phase relationships between millennial-scale events 64 000–24 000 years ago, Paleoceanography, 15, 565–569, 2000.
Siddall, M., Rohling, E. J., Almogi-Labin, A., Hemleben, C., Meischner, D., Schmelzer, I., and Smeed, D. A.: Sea-level fluctuations during the last glacial cycle, Nature, 423, 853–858, 2003.
Siddall, M., Rohling, E. J., Thompson, W. G., and Waelbroeck, C.: MIS 3 sea level fluctuations: data synthesis and new outlook, Rev. Geophys., 46, RG4003, doi:10.1029/2007RG000226, 2008.
Sierro, F. J., Hodell, D. A., Curtis, J. H., Flores, J. A., Reguera, I., Colmenero-Hidalgo, E., Bárcena, M. A., Grimalt, J. O., Cacho, I., Frigola, J., and Canals, M.: Impact of iceberg melting on Mediterranean thermohaline circulation during Heinrich events, Paleoceanography, 20, PA2019, doi:10.1029/2004PA001051, 2005.
Sierro, F. J., Andersen, N., Bassetti, M. A., Berné, S., Canals, M., Curtis, J. H., Dennielou, B., Flores, J. A., Frigola, J., Gonzalez-Mora, B., Grimalt, J. O., Hodell, D. A., Jouet, G., Pérez-Folgado, M., and Schneider, R.: Phase relationship between sea level and abrupt climate change, Quaternary Sci. Revi., 28, 2867–2881, 2009.
Skinner, L. C., Elderfield, H., and Hall, M.: Phasing of millennial climate events and Northeast Atlantic deep-water temperature change since 50 ka BP, in: Ocean Circulation: Mechanisms and Impacts, edited by: Schmittner, A., Chiang, J. C. H., and Hemming, S. R., AGU Geophysical Monograph Series 173, Washington, D. C., 197–208, 2007.
Svensson, A., Andersen, K. K., Bigler, M., Clausen, H. B., Dahl-Jensen, D., Davies, S. M., Johnsen, S. J., Muscheler, R., Parrenin, F., Rasmussen, S. O., Röthlisberger, R., Seierstad, I., Steffensen, J. P., and Vinther, B. M.: A 60 000 year Greenland stratigraphic ice core chronology, Clim. Past, 4, 47–57, doi:10.5194/cp-4-47-2008, 2008.
Tesson, M., Gensous, B., Allen, G. P., and Ravenne, C.: Late quaternary deltaic lowstand wedges on the Rhône continental shelf, France, Mar. Geol., 91, 325–332, 1990.
Tesson, M., Posamentier, H. W., and Gensous, B.: Stratigraphic organization of late pleistocene deposits of the western part of the Golfe du Lion shelf (Languedoc shelf), Western Mediterranean Sea, using high-resolution seismic and core data, Am. Assoc. Petrol. Geol. (AAPG) B., 84, 119–150, 2000.
Thompson, W. G. and Goldstein, S. L.: Open-system coral ages reveal persistent suborbital sea-level cycles, Science, 308, 401–404, 2005.
Thompson, W. G. and Goldstein, S. L.: A radiometric calibration of the SPECMAP timescale,

CPD
7, 4401–4428, 2011

Quaternary Sci. Rev. 25, 3207–3215, 2006.
Ulses, C., Grenz, C., Marsaleix, P., Schaaff, E., Estournel, C., Meulé, S., and Pinazo, C.: Circulation in a semi-enclosed bay under influence of strong freshwater input, J. Mar. Syst., 56, 113–132, 2005.
Vail, P. R., Mitchum Jr., R. M., Todd, R. G., Widmier, J. M., Thompson III, S., Sangree, J. B., Bubb, J. N., and Hatleid, W. G.: Seismic stratigraphy and global changes of sea level, in: Seismic Stratigraphy – Applications to Hydrocarbon Exploration, edited by: Payton, C. E., The American Association of Petroleum Geologists, Tulsa, 49–212, 1977.
Waelbroeck, C., Labeyrie, L., Michel, E., Duplessy, J. C., McManus, J. F., Lambeck, K., Balbon, E., and Labracherie, M.: Sea-level and deep water temperature changes derived from benthic foraminifera isotopic records, Quaternary Sci. Rev., 21, 295–305, 2002.
Yokoyama, Y., Esat, T. M., and Lambeck, K.: Coupled climate and sea-level changes deduced from Huon Peninsula coral terraces of the last ice age, Earth Planet. Sci. Lett., 193, 579–587, 2001.

CPD
7, 4401–4428, 2011

New insights into MIS 3 sea level variability

J. Frigola et al.

Table 1. Additional tie points for the tuning of the *G. bulloides* $\delta^{18}O$ record from PRGL1-4 borehole to the SPECMAP isotope stack (Martinson et al., 1987) for the 270–530 kyr time-interval. 29 ^{14}C-AMS dates on calcareous shells confirm the chronology achieved by tuning the $\delta^{18}O$ record from PRGL1-4 to NGRIP for the last 120 ka (Sierro et al., 2009).

Event	PRGL1-4 depth (m)	Age SPECMAP (kyr)
Top MIS 8.5	157.10	279.00
MIS 8.5	158.00	286.00
Base 8.5	158.30	292.00
Top 9.1	159.10	304.00
Base MIS 9.1	159.50	312.00
MIS 9.3	161.40	331.00
TIV	163.90	341.00
Top 11.1	196.10	370.00
Base MIS 11.1	196.76	377.00
Base 11.1	197.11	380.13
Top 11.3	198.37	386.30
Minimum in 11.3	199.33	405.21
TV	199.95	419.00
Top 13.1	289.41	475.00
MIS 13.2	295.02	513.00
Base 13.3	300.97	530.00

CPD
7, 4401–4428, 2011

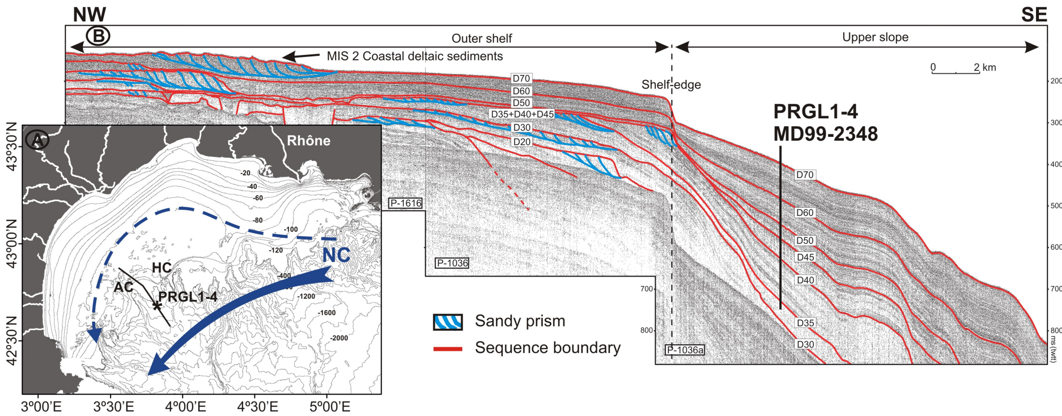

Fig. 1. **(A)** Bathymetric map of the Gulf of Lion with location of borehole PRGL1-4 in the interfluve separating Aude and Hérault submarine canyons, AC and HC, respectively. The dominant component of the general circulation is shown by the geostrophic Northern Current (NC), which flows southwestward along the slope and occasionally penetrates over the outer shelf, blue arrows. **(B)** Part of high-resolution seismic reflection profile P-1036a crossing the borehole location in a NW-SE direction across the outer shelf and upper slope (modified from Jouet, 2007). Stratigraphic sequences S1 to S5 delimited by main reflectors D35 to D70 marked as defined by Jouet (2007). Red reflectors show the main conformities separating RPUs while the blue ones correspond to sandy prisms.

CPD
7, 4401–4428, 2011

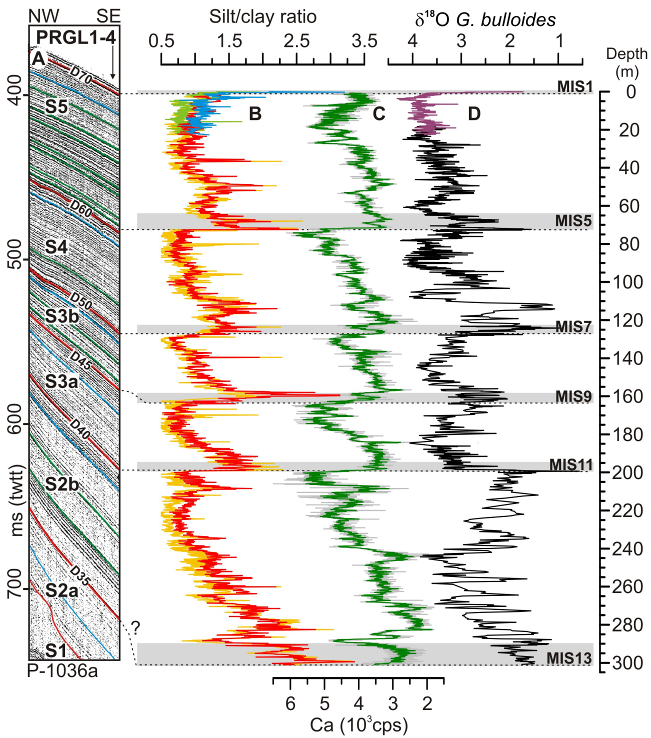

Fig. 2. **(A)** Close view of high-resolution seismic reflection profile P-1036a at the location of borehole PRGL1-4 (Jouet, 2007). **(B)** Silt/clay ratio records from total (light orange and green) and Ca-free (red and blue) sediment fractions from PRGL1-4 and MD99–2348 sediment cores, respectively. **(C)** 5-point moving average (green) of Ca record (grey) from PRGL1-4. **(D)** Oxygen isotopic records from PRGL1-4 (black) and MD99-2348 (purple) obtained from *G. bulloides*. Grey bars correspond to condensed interglacials sequences 1, 5, 7, 9, 11 and 13. Dotted lines correlate the main seismic reflectors (sequence boundaries) and their expression on the different records.

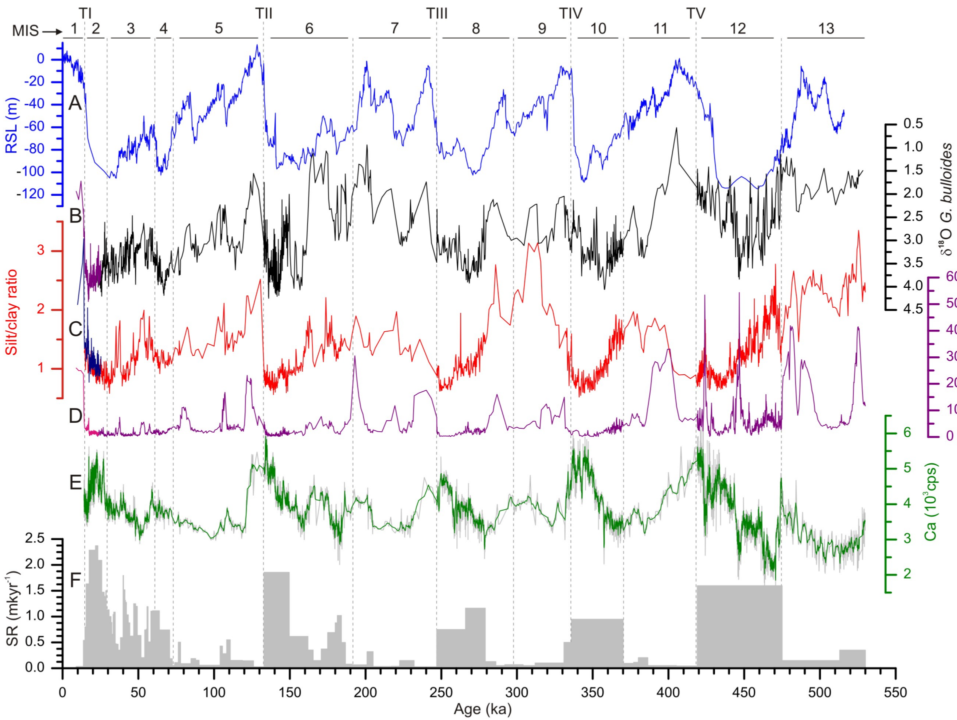

Fig. 3. Multiproxy continuous records of PRGL1-4 borehole with respect to relative sea level oscillations for the last 500 ka. **(A)** Composite Central Red Sea relative sea level reconstruction for the last 500 ka (Rohling et al., 2009). PRGL1-4 records of **(B)** *G. bulloides* δ^{18}O, **(C)** silt/clay ratio, **(D)** total fine sand (%) from Sierro et al. (2009), **(E)** XRF-Ca, and **(F)** linear sedimentation rates. The top 22 ka of the *G. bulloides* δ^{18}O record (purple), the silt/clay ratio of the carbonate-free fraction (blue) and the total fine sand (pink) are from overlapping core MD99-2348, which include the abrupt change associated with the last deglaciation that is not covered by the XRF-Ca record of PRGL1-4.

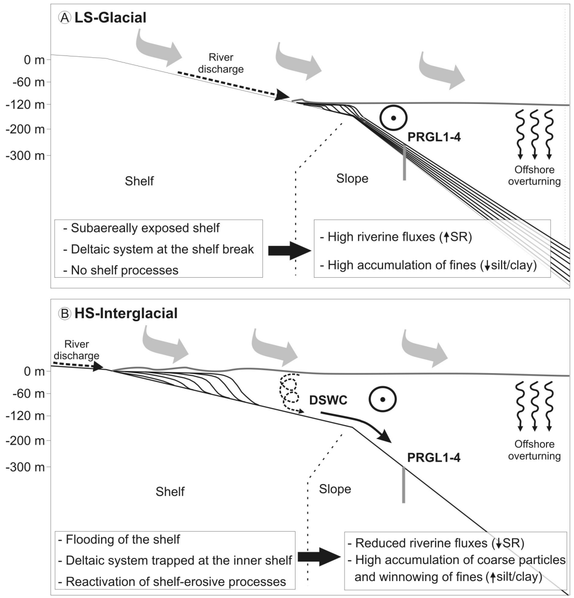

Fig. 4. Conceptual depositional model of the Gulf of Lion continental margin at orbital scale. **(A)** During the lowstand (LS) depositional mode (glacial periods) the continental shelf is subaerially exposed and the basinwards migration of deltaic system results in high amounts of fine particles supplied directly to the upper slope. **(B)** Flooding of the shelf during the high-stand (HS) depositional mode (interglacial periods) traps deltaic systems in the inner shelf, thus disconnecting the upper slope from direct fluvial discharges. Moreover, the creation of a relatively thin layer of water over the continental shelf reactivates shelf erosive processes, such as Dense Shelf Water Cascading (DSWC), that are able to transport coarse particles down the slope. Both processes contribute to generate thin condensed layers (CLs) in the upper slope. Grey arrows represent the northern winds involved in cooling the superficial shelf water for dense shelf water formation and offshore overturning. Dot in a circle shows the dominant direction of the slope-parallel Northern Current. The discontinuous spiral arrow over the shelf represents shelf-erosive processes, as DSWC.

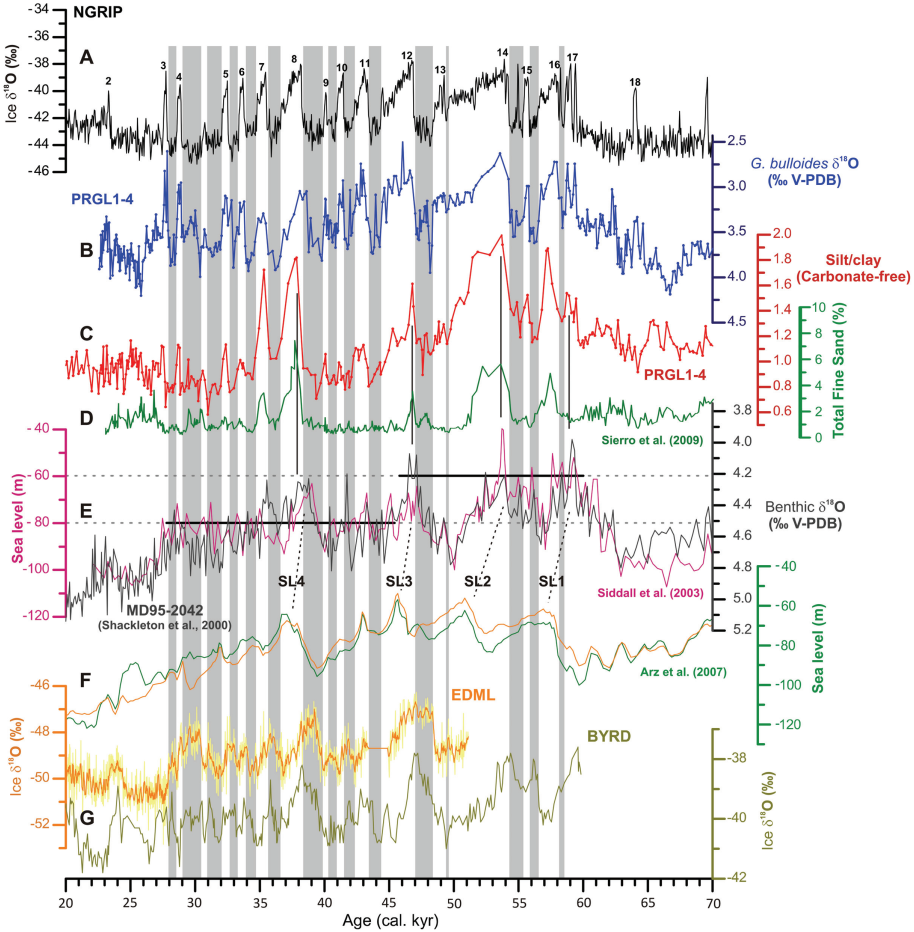

Fig. 5. Caption on next page.

Fig. 5. Comparison of different records of climate variability and sea level reconstructions for the MIS 3 period all of them age-scaled to the Greenland ice core NGRIP (Svensson et al., 2008) **(A)**. **(B, C and D)** *G. bulloides* oxygen isotopic record (blue), silt/clay ratio (red) and total fine sand fraction from PRGL1-4 borehole, respectively. **(E)** Benthic oxygen isotopic record from MD95-2042 (Shackleton et al., 2000) (dark grey) compared to Red Sea sea level reconstruction by (Siddall et al., 2003) (pink), with horizontal lines showing that mean sea level was ~ 20 m higher in early MIS 3 than in late MIS 3. Discontinuous lines point four millennial-scale peaks of relative high sea level (SL1, 2, 3 and 4). **(F)** Sea level reconstructions from the Northern Red Sea based on two different temperature corrections for the deep basin (Arz et al., 2007). **(G)** Oxygen isotopic records from Antarctic ice cores EDML and BYRD (Blunier and Brook, 2001; EPICA, 2006) CH_4-synchronized to Greenland ice core NGRIP (Svensson et al., 2008). Numbers above the NGRIP record represent warm GIS while vertical grey bars correspond to cold GS and HE.